Study on Dielectric Breakdown at DC Polarity Reversal in Oil / pressboard-composite Insulation System

T. Nara, K. Kato, F. Endo and H. Okubo
Nagoya University, Nagoya, JAPAN
nara@okubo.nuee.nagoya-u.ac.jp

***Abstract*- By using Kerr electro-optic method, charge behavior in oil / pressboard (PB) composite insulation system, which is the basic insulation structure of a transformer, was investigated under DC voltage. Right after the DC voltage application, electric field became the capacitive distribution, and had a strong value which was determined by permittivity of materials. The field strength decreased gradually with time as charge in oil was accumulated on PB. When the voltage polarity was reversed, the applied electric field was superimposed by the electric field formed by the accumulated charge on PB, and very strong field appeared right after the polarity reversal. This could cause the discharge in the oil gap even when the independent applied voltage was insufficient to initiate discharge. It was found out that the critical value of the discharge initiation at the polarity reversal was determined by the breakdown field strength of the oil gap.**

I. Introduction

Oil immersed transformers are being widely used in electric power systems, and achieve the stable large electric power supply. Recently, further compactness and larger capacity are required. To realize these, many studies have been performed about initiation and propagation of discharge in oil [1-5]. Moreover, as clarification of charge behavior is important for the realization of the reasonable insulation design and high-reliability of transformers, the flow electrification has been studied [6]. Today, quantitative clarification of breakdown phenomena in an oil / PB composite insulation system is demanded based on the in-situ measurement of the change of electric field strength in oil caused by charge accumulation on PB.

In this paper, PB was placed on the parallel plane electrode, and electric field strength E in the oil gap between PB and an electrode was measured with Kerr electro-optic method [7, 8]. After applying DC voltage for sufficiently long time, the voltage polarity was reversed to initiate discharge in the oil gap. Prestress DC voltage applied before the polarity reversal was changed, and discharge initiation condition at the polarity reversal was examined. Through these experiments, the influence of the accumulated charge on PB on the discharge initiation was quantitatively clarified.

II. Behavior of Electric Field in HVDC Equipment

Operating voltage of HVDC equipment is sometimes reversed in its polarity as shown in Fig. 1. Such equipment will be exposed to not only constant DC voltage but also sudden voltage change at turn-on (Fig. 1 (a)), DC polarity reversal (Fig. 1 (b)) and turn-off (Fig. 1 (c)). At the time (b) and (c), accumulated charge on the solid insulator greatly influenced electric field distribution in HVDC equipment. Especially, for time (b), electric field formed by the accumulated charge on solid insulator can be superimposed to the applied field, and strong electric field can appear at a certain place in equipment. Therefore, the DC polarity reversal could be very severe for HVDC insulation of equipment.

Figure 2 shows examples of potential distribution lines under AC or DC voltage. Their potential distribution is quite different. At the instant of turn-on, potential lines distribute uniformly in the oil gap. On the other hand, under DC voltage, most of the potential distribute in PB. At the instant of the polarity reversal, complex potential distribution appears.

Systematic studies on the transient electric field measurement

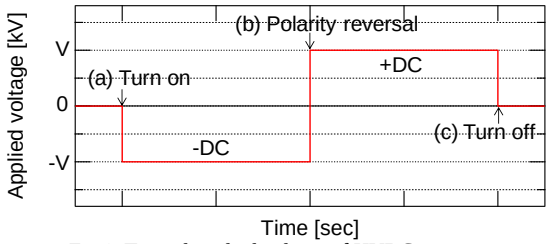

Fig.1. Typical applied voltage of HVDC equipment.

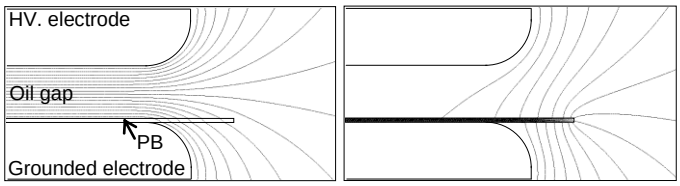

(a) AC voltage (b) DC votage

Fig. 2. Equipotential lines under AC and DC voltage.

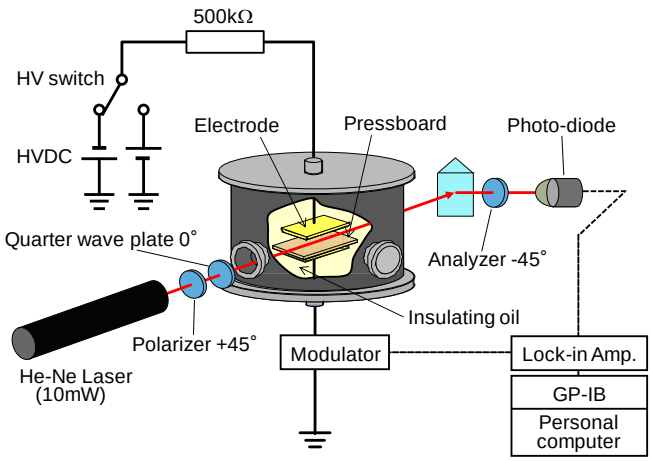

Fig.3. Experimental setup for electric field measurement in insulating oil using Kerr electro-optic technique.

and its relation with discharge at the DC voltage polarity reversal have been insufficient. Quantitative understandings of charge behavior and discharge initiation criteria are inevitable to achieve the reasonable insulation design of HVDC equipment with high performance and high reliability.

III. Behavior of Electric Field at Polarity Reversal

A. *Experimental setup for Kerr electro-optic field measurement*

Figure 3 shows the setup for Kerr electro-optic field measurement in insulating oil. This method has an advantage of the electric field measurement without any disturbance. A circularly polarized He-Ne laser beam passes through the electrically stressed insulating oil in the test cell. The Kerr effect is caused by changes of polarization under an applied electric field and the Kerr constant is the specific constant of the material. The relationship between the light intensity ratio $I_{1\omega}/I_{dc}$ and average applied field strength E_{dc} is expressed by the following equation (1) [7, 8, 9].

$$I_{1\omega} / I_{dc} = 4\pi BLE_{dc}E_{ac} \quad (1)$$

where $I_{1\omega}$ is light intensity (first harmonic), I_{dc} is light intensity (dc), B is Kerr constant, L is electrode length and E_{ac} is the applied electric field (ac). The Kerr constant was obtained as 1.43×10^{-15} m/V^2 in mineral oil.

Figure 4 shows an oil / PB composite insulation system for electric field measurement. In a parallel plane electrode, a PB (thickness of 0.8 mm) was placed on the lower electrode. It was grounded via a modulator. The upper electrode was connected to the high voltage switch, and the polarity of the applied DC voltage could be reversed in 40 msec. Temporal change of E at the center of the oil gap was measured at various DC voltages. And after applying the DC voltage for sufficiently long time, the voltage polarity was reversed to the opposite one. During this process, the value of E in the oil gap was continuously measured at the center of the oil gap.

All experiments were carried out at room temperature. Moisture in mineral oil was kept at 10~20 ppm, and was degassed after each experiment. Properties of the mineral oil and PB are listed in Table 1.

B. *Electric field measurement at un polar DC voltage*

Figure 5 (a) shows the time dependence of electric field strength in the oil gap of Fig. 4. Electric field strength decreased with time at both voltage polarities, and the decay of field strength at -10 kV was faster than at +10 kV. From the measured value of E, the charge density q_a accumulated on PB can be calculated based on the following continuity relation (2) of dielectric flux density.

$$\varepsilon_0\varepsilon_{oil}E_{oil} + q_a = \varepsilon_0\varepsilon_{PB}E_{PB} \quad (2)$$

where ε_0 is the dielectric constant in vacuum, ε_{oil} and ε_{PB} are relative dielectric constants of oil and PB, E_{oil} and E_{PB} are electric field strength in oil and PB.

Figure 5 (b) shows calculated results of q_a. Charge accumulation on the PB / oil interface was faster at -10 kV than at +10 kV. This is explained by the ability of negative charge adsorption of PB [9].

C. *Electric field measurement at polarity reversal*

Figure 6 shows the change of the electric field strength in the oil gap (Fig. 3 (a)) with time when the polarity of applied voltage was reversed. Electric field strength in the oil gap gradually decreased during the pre-stress period of DC voltage, and was almost equal to 0 kV/mm after 200 seconds. As electric field strength sufficiently attenuated at 2000 seconds, the voltage polarity was reversed from +10 kV to -10 kV or -10 kV to +10 kV. At the instant of the polarity reversal, the capacitive electric field by the reversed voltage was superimposed by the field formed by the accumulated charge on PB, and the resultant electric field strength was enhanced to about twice that of applied one.

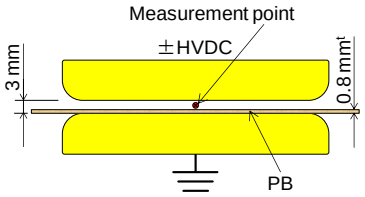

Fig.4. Electrode configuration.

Table 1. Properties of the mineral oil and PB.

	Mineral oil	PB
Relative permittivity at 80°C	2.2	4.4
Volume resistivity (Ω·cm)	3.0×10^{13}	$\leqq10^{16}$

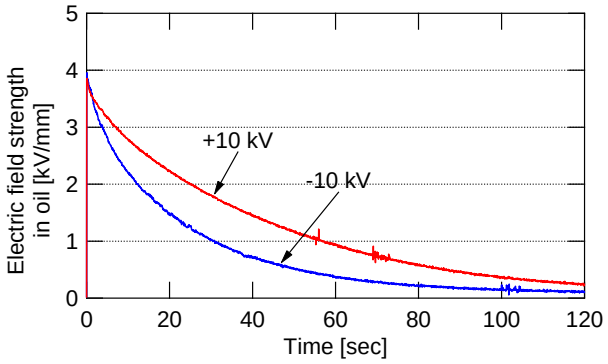

(a) Electric field strength

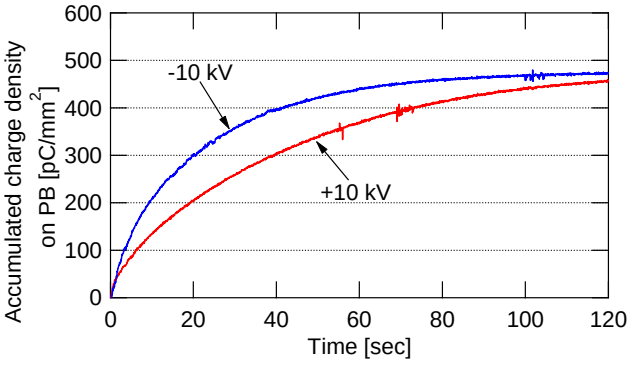

(b) Charge density on PB

Fig.5. Time dependence of electric field strength, charge density on PB in mineral oil.

D. *Charge behavior and its influence on electric field strength*

This phenomenon is schematically described in Figure 7. The equivalent circuit of an oil / PB composite insulating system is shown in Figure 8. At the instant of the negative DC voltage application, E was dominated by the capacitance, i.e. permittivity of the oil gap and PB, and expressed with equation (3).

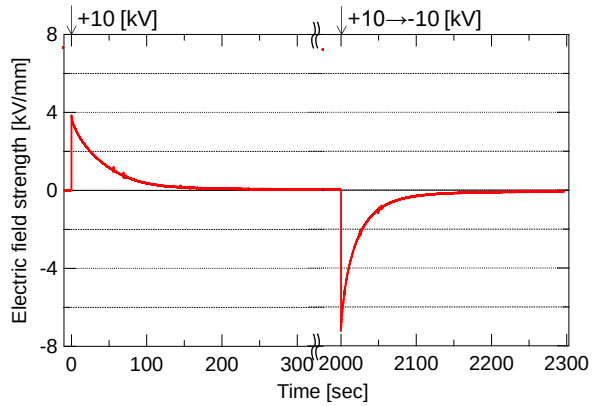

(a) +10 kV to -10 kV

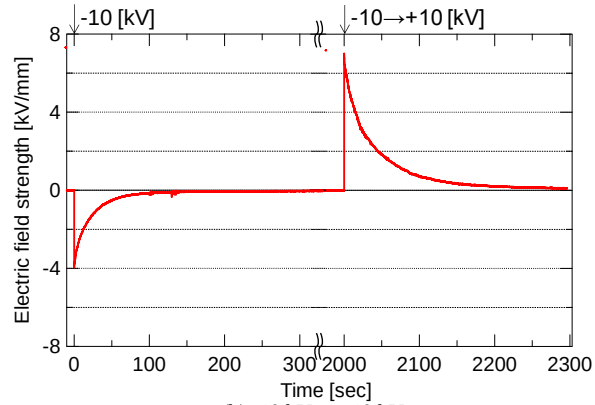

(b) -10 kV to +10 kV

Fig.6. Time dependence of electric field strength at polarity reversal.

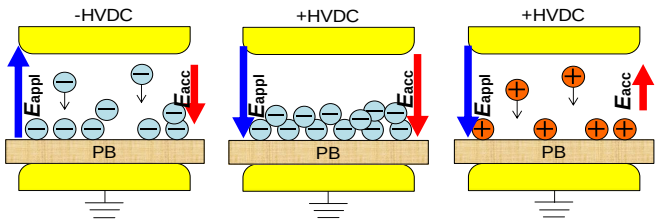

(a) At prestress period (b) At the instant of polarity reversal (c) After the polarity reversal

Fig.7. Schematic illustration of charge behavior in mineral oil.

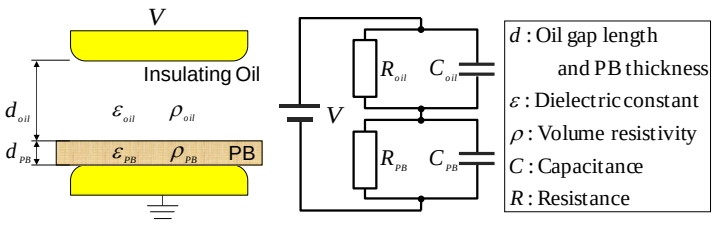

(a) Insulation configuration (b) Equivalent circuit

Fig. 8. Equivalent circuit of oil / PB composite insulating system.

$$E_i = \frac{C_{PB}}{C_{oil}+C_{PB}}\frac{V}{d_{oil}} = \frac{V}{d_{oil}+{\varepsilon_{oil}}/{\varepsilon_{PB}}\,d_{PB}} \tag{3}$$

And then the value of E decreased with time due to the negative charge accumulation on PB (Fig. 7 (a)). Finally, it reached to the stable value which was determined by the resistivity [9], and is given with equation (4).

$$E_s = \frac{R_{oil}}{R_{oil}+R_{PB}}\frac{V}{d_{oil}} = \frac{V}{d_{oil}+{\rho_{PB}}/{\rho_{oil}}\,d_{PB}} \tag{4}$$

Just after the polarity reversal, the applied field was superimposed by the electric field generated by the negative charge accumulated on PB (Fig. 7 (b)). After the polarity reversal, positive charges were gradually accumulated on the PB, and electric field strength decreased (Fig. 7 (c)). Since pre-stress voltage was applied for sufficient long time and the amount of accumulated charge was saturated, resultant electric field strength in the oil gap was almost equal at both polarities just after the polarity reversal.

Figure 9 shows the schematic diagram of electric field in the oil gap when the voltage polarity is reversed from V_{pre} to V_{rev}. The coordinate axes of E_{acc} and E_{appl} are shown inversely to help understanding. E_{acc} and E_{appl} are proportional to V_{pre} and V_{rev}, respectively. From this figure, it is easy to understand that even if V_{pre} is not high, E could be very strong owing to E_{acc} just after polarity reversal.

IV. Breakdown Characteristics at Porarity Reversal

A. *AC and DC breakdown characteristics*

It is well known one minute AC breakdown field strength E_{BD} in the oil gap is expressed with the equation (5).

$$E_{BD} = Kd^{-a} \tag{5}$$

where d is oil gap length, K and a are constants (K=20~23, a=0.30~0.33).

DC breakdown field strength of mineral oil used in this study was measured with parallel plane electrode (gap length: 2.2 mm). The mean breakdown field strength E_{BD} was 24.6 kV/mm and standard deviation was 3.52kV/mm. This value is nearly equal to that for AC peak.

B. *Breakdown behavior at polarity reversal*

The value of the polarity reversed voltage was changed under various pre-stress voltages of -10 kV to -50 kV, and discharge inception voltage in the oil gap was measured. Experimental results are shown in Figure 10. The lower and upper horizontal axes show E_{acc} and q_a, respectively, and the vertical axis E_{appl}. The value of q_a was calculated with eq. (2). "○" marks in the figure show occurrence of discharge at the polarity reversal, and the "×" marks indicate no-occurrence of discharge. The figure suggests that there is a critical boundary between discharge and no discharge. In the former section, E_{BD} was clarified to be 24.6 kV/mm in the oil gap of 2.2 mm. The relation between E_{appl} and E_{acc}, which satisfy this E_{BD}, is plotted as a solid line. The solid line coincides well with the above mentioned boundary. This result suggests that when the sum of E_{acc} and E_{appl} exceeds E_{BD}, discharge starts in the oil

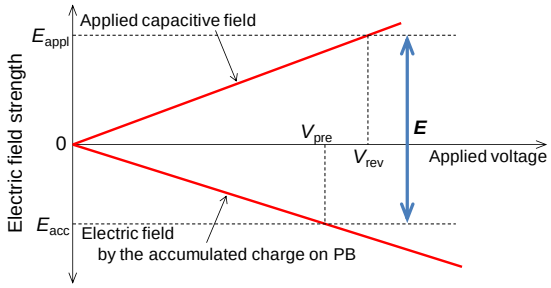

Fig.9. Schematic diagram of electric field at polarity reversal.

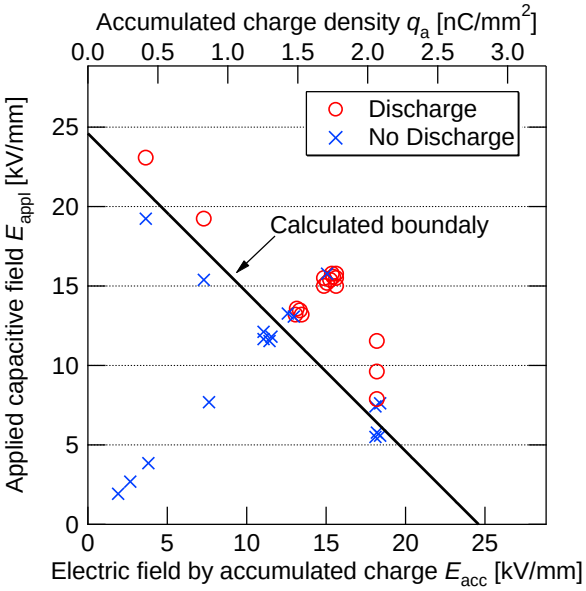

Fig.10. Discharge initiation characteristics in oil / PB insulation system at the polarity reversal test.

gap in a oil / PB composite insulation system.

Once discharge initiated in the oil gap, it propagated as surface discharge on PB. Figure 11 (a) shows its side view of the examined specimen in Fig. 4. Figure 11 (b) and (c) show the discharge propagation along the PB surface at the polarity reversal (-40 kV to +40 kV). Discharge appeared at several places intermittently for several seconds.

IV. Conclusions

In an oil / PB composite insulation system, electric field strength in mineral oil was measured in situ with Kerr electro-optic method, and the accumulated charge density on PB was estimated. Considering electric field strength generated by the accumulated charge on PB, the critical electric field strength of discharge inception in the oil gap was derived. Following results were obtained;

(1) The electric field in the oil gap became strong owing to the capacitive distribution just after the voltage application, and then after that, decreases gradually because of the charge accumulation on PB.

(2) Just after the polarity reversal, the electric field strength in the oil gap became the sum of the electric field formed by the accumulated charge and the applied electric field. Its value was about twice that at beginning of voltage application in the case where the voltage level is equal before and after the polarity reversals.

(3) Discharge at the polarity reversal initiated when the sum of the electric field formed by the accumulated charge on PB and the applied field exceeded the breakdown electric field strength of the oil gap.

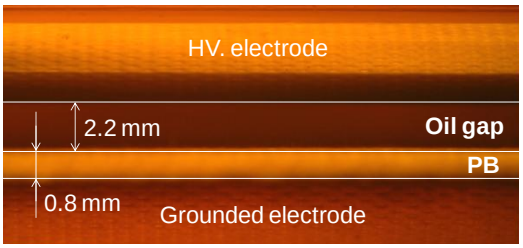

(a) Side view

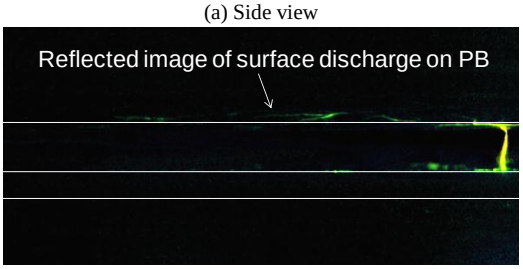

(b) Discharge in the oil gap at -40 kV → +40 kV

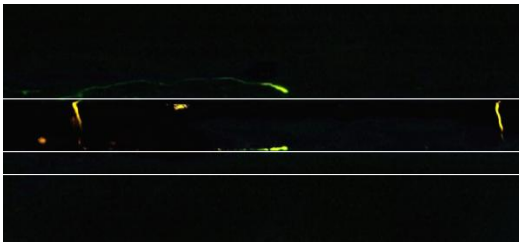

(c) Discharge in the oil gap at -40 kV → +40 kV

Fig.11. Discharge appeared at DC polarity reversal in an oil / PB composite insulation system.

References

[1] A. Atten and A. Saker, "Streamer Propagation over a Liquid/Solid Interface", IEEE Trans. on Elect. Insul., Vol. 28, No. 2, pp. 230-242, 1993.

[2] N. K. Bedoui, A. Beroual and F. Chappuis, "Creeping Discharge on Solid/Liquid Insulating Interface under AC and DC Voltages", IEEE CEIDP, pp. 784-787, 2000.

[3] R. Hanaoka, T. Kohrin, T. Miyagawa and T. Nishi, "Creepage Discharge Characteristics over Solid-Liquid Interfaces with Grounded Side Electrode", IEEE Trans. on Diele. and Elect. Insul., Vol. 9, No. 2, pp. 308-315, 2002.

[4] L. Kebbadi and A. Beroual, "Optical and electrical investigation on creeping discharge over solid/liquid interfaces under impulse voltage", IEEE ICDL, pp. 131-134, 2005.

[5] H. Yamamoto, S. Uozaki, R. Hanaoka, S. Takata, Y. Kanamaru and Y. Nakagami, "Creeping Discharge in Transformer Oil under Lightning Impulse Voltage over 100 kV Peak Value", IEEE ICDL, pp. 130-133, 2008.

[6] M. Wakamatsu, N. Inoue, K. Kato, H. Koide and H. Okubo, "Charge Behavior in Flowing Oil in Oil / Pressboard Insulation System by Electro-Optic Field Measurement", IEEE Trans. on Diele. and Elect. Insul., Vol.. 10, No. 6, pp. 956-962, 2003.

[7] K. Kato, Y. Hashiba, Y. Nakagami, M. Miyamoto and H. Okubo, "Study on Charge Behavior in Flowing Transformer Oil / Pressboard Composite Insulation System Using Electro-Optic Field Measurement," IEEE ICDL, pp. 349-352, 1999.

[8] S. Yamamoto, K. Kato, F. Endo, Y. Hatta, H. Koide and H. Okubo: "Kerr Electro-Optic Field Measurement in Palm Oil Fatty Acid Ester Transformer Insulation System", IEEE CEIDP, pp. 748-787, 2007.

[9] M. Hikita, A. Sawada, K. Kato and H. Okubo, "Optical Measurement of Electric Field in Transformer Oil / Pressboard Composite Insulation System and Discussion on Charge Dynamics", IEEE ICPADM, pp. 298- 302, 1997.